Aerodynamic Behavior of an Ornithopter Capable of a Sustained and Controlled Flight

Bernard Adaramola
Department of Mechanical & Mechatronics Engineering,
Afe Babalola University,Ado Ekiti Nigeria.
adaramolaba@abuad.edu.ng

Adedotun Adetunla
Department of Mechanical & Mechatronics Engineering,
Afe Babalola University,Ado Ekiti Nigeria.
dotunadetunla@yahoo.com

Adeyinka Adeoye
Department of Mechanical & Mechatronics Engineering,
Afe Babalola University,Ado Ekiti Nigeria.
aadeoye@abuad.edu.ng

Abstract

An Ornithopter is a device that mimics the flights of birds by flapping its wings. Aircraft can fly at immense speeds and in harsh conditions, but to an extent, they lack the level of maneuverability seen in birds and insects. This work delves into the control and automation for stability of flapping wing flight due to its advantages over fixed wing fliers like increased maneuverability and its contribution to research and society. To ensure the model stays airborne and for the wings to create lift equal to the weight of the Ornithopter, the design and selection of the components was carried out to meet the desired performance requirements of an Ornithopter which stems from the features of bird flight such as good maneuverability, low speed flight capability, agility, and high propulsive efficiency. The Ornithopter was built from materials commonly sourced and modelled by using SolidWorks simulation.

Keywords
Aerodynamic Simulation, Automation, Ornithopter, Wing Mechanism

1. Introduction

A Flapping Wing Unmanned Aerial Vehicle is also known as an Ornithopter, the name is derived from two Greek words, ‘Ornithos’ meaning bird and ‘pteron’ meaning wing. An Ornithopter is a device that flies by flapping its wings. It imitates the flight of creatures in nature mainly birds and insects (Rawat et al. 2013). Though these devices may differ in form, they are built on the same scale as the creatures they imitate. The wings generate the required lift and thrust required for flight via a flapping mechanism which converts the rotary motion of the motors through the gears into oscillating motion of the wings. The principle of operation of the Ornithopter is same as the airplane; the forward motion through the air allows the wings to deflect air downward, producing lift (Dubey et al. 2017). The flapping motion of the wings takes the place of rotating propeller. Engineers and researchers have experimented with wings that require carbon fiber, plywood, fabric, ribs, and the trailing edge to be stiff, strong, and for the mass to be as low as possible. Unlike airplanes and helicopters, the driving airfoils of the Ornithopter have a flapping or oscillating motion, instead of rotary motion (Singhal et al. 2018). As with helicopters, the wings usually have a combined function of providing both lift and thrust. Theoretically, the flapping wing can be set to zero angle of attack on the upstroke, so it passes easily through the air. Since typically the flapping airfoils produce both lift and thrust, drag – inducing structures are minimized. These two advantages potentially allow a high degree of efficiency (Bhargava 2014).

1.1 Objectives

Many ornithopter designs still fail to fly despite the rapidly increasing population building electric ornithopters. A major problem in most designs is an inability to generate enough lift to take off in the first place (Abel et al. 2014). This precludes additional flight research, such as maneuverability, flight distance or time and this coupled with weight and cost constraints. To stay airborne, the wings must create lift equal to the weight of the Ornithopter. Thus, there arises the need for the design and selection of the components to meet the desired performance requirements of an Ornithopter which stems from the features of bird flight such as good maneuverability, low speed flight capability, agility, and high propulsive efficiency. This paper presents the schematic of an ornithopter, with adequate flight stability, which could serve as a baseline for manufacturers of Unmanned Aerial Vehicles (UAV) and increase the applicability of UAV in Industries.

2. Literature Review

Several attempts at building flapping robots or ornithopters have been made (Bento 2017 and Box 2017). The first reasonably successful of these tests occurred some thousand years later in 1060, when a monk managed to glide approximately 200 yards before his predictably destructive (though non-fatal) encounter with the ground (Sanderson et al. 2016). A notable step forward in ornithopter design came from Leonardo Da Vinci, although it was never properly investigated until the 19th century (Sanderson et al. 2016). Leonardo da Vinci began to study the flight of birds) (Srigrarom 2015). He grasped that human are too heavy, and not strong enough, to fly using wings simply attached to the arms. Therefore, he sketched a device in which the aviator lies down on a plank and works two large, membranous wings using hand levers, foot pedals, and a system of pulleys (Sail et al. 2016). The first ornithopters capable of flight were constructed in France Jobert in 1871 used a rubber band to power a small model bird (De Croon 2009). Cron et al also made rubber-powered ornithopters during the 1870s Tatin's ornithopter was perhaps the first to use active torsion of the wings, and apparently it served as the basis for a commercial toy offered by Pichancourt C. 1889. Gustave Trouve was the first to use internal combustion and his 1890 model flew a distance of 70 metres in a demonstration for the French Academy of Sciences (Bhargava 2015). The wings were flapped by gunpower charges activating a bourbon tube. While some were successful, many neither take off nor fly only for a short duration due to their higher complexity or poor design.

3. Methods

Flight is a phenomenon that has long been a part of the natural world. Birds' fly not only by flapping their wings and gliding with their wings outstretched for long distances but based on principles of physical science. The ornithopter must be heavier than the air flight, which is made possible by the balance of the four fundamental forces: lift, thrust, drag and weight. These four forces act directly on the flying model as shown in Figure 1.

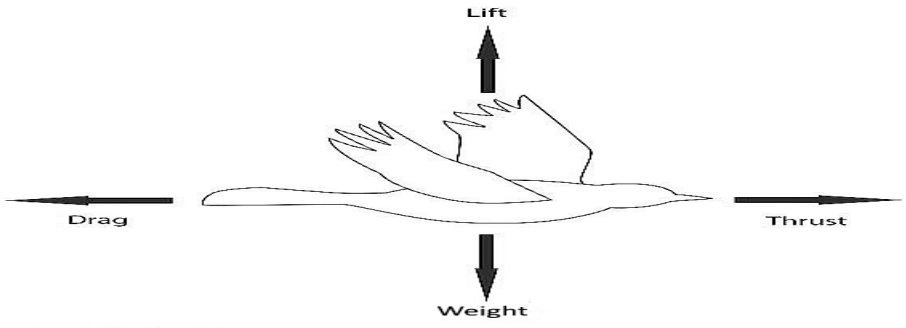

Figure 1. The Four Forces Acting on a Bird

3.1 Materials Design

The materials selected for the Ornithopter fuselage, other mechanical components, and its attachments to it were selected based on the following criteria according to Rawat et al: Weight, Strength, Cost, Fuselage Frontal Area, Shape.

3.2Material Dimension

Wings: Wings are the most important parts of the model which can determine the flight characteristics of the Ornithopter. The sizes of a medium sized Ornithopter range between 30cm to 2m (Table 1). The wingspan (*b)* set for the ornithopter is 124cm and Chord length *(c)* is 21cm. The shape of the wing is elliptical, and the wing area *(S)* is found using the formula below:

$$Wing\ Area\ (S) = a \times b \times \pi$$

where,
$a = wing\ span\ \div 2 = 124 \div 2 = 62$
$b = root\ chord\ \div 2 = 21\ \div 2 = 10.5$
$Wing\ Area\ (S) = 62 \times 10.5 \times \pi = 2044.14\ cm^2$

Aspect ratio and wing loading come here under careful considerations. Wing Aspect Ratio (*AR*) can tell the manoeuvrability of any bird. It is simply the ratio of the square of the wingspan (*b)* to the wing area *(S)*

$$AR = {b^2}/{S}$$
$$= {124^2}/{2044.14} = 7.5$$

The higher the wing loading, faster the bird must fly to overcome its weight force (gravity)[13]. Wing Loading is simply the ratio of weight *(W)* to wing area (*S)*
Weight *(W)* in kilograms for which the intended model is set not to exceed 2kg (2000g), this includes all electrical and mechanical components.

$$Wing\ Loading = {W}/{S}$$
$$= {750}/{2044.14}$$
$$= 0.387 g/cm^2$$

Flapping Frequency to be generated for model is also set to be between 2-5 Hz.
First, the constants were set.

- Coefficient of Drag (C_D) = 2 (Based on airfoil type)
- Density of air (**ρ**) = 1.225 kg/m^3
- Acceleration due to gravity (G) = 9.81 m/s^2
- Maximum angle wing makes with respect to body (**θ**) = 0.5236 radians

Finally, values were calculated and presented in Table 1

- Drag force (F_d)
  $F_d = \rho \times C_d \times c \times {b^3}/{3}$
  $= 1.225 \times 2 \times 0.21 \times {1.24^3}/{3}$
  $= 0.33\ N$

- Angular Momentum (***ω***)
  $\omega = {\sqrt{M \times G}}/{F_d}$
  $= {\sqrt{0.75 \times 9.81}}/{0.33}$
  $= 4.72\ rad/s$
- The time for the downstroke (*T)*
  $T = {1}/{(\omega \times \theta)^2}$
  $= {1}/{(4.72 \times 0.5236)^2}$
  $= 0.16\ s$
- The torque (τ) of the wings
  $\tau = \rho \times \omega^2 \times C_d \times c \times {b^4}/{8}$
  $= 1.225 \times 4.72^2 \times 2 \times 0.21 \times {1.24^2}/{8}$

$= 3.4\ Nm$

- Power (P) in watts
  $P = \tau * \omega$
  $= 3.4 \times 4.72$
  $= 16.04\ W$

- Power (P_{hp}) in horsepower
  $P_{hp} = P * 0.00134102$
  $= 16.04 \times 0.00134102$
  $= 0.022$

Table 1. Values of the Ornithopter Wing

b (m)	M (kg)	c (m)	F_d (N)	ω (rad/s)	T (s)	τ (Nm)	P (W)	P_{hp}
1.24	0.75	0.21	0.33	4.72	0.16	3.4	16.93	0.022

3.3 Material Fabrication

The fabrication of the mechanical components of the Ornithopter was carried out by making the engineering drawing using SolidWorks, and the fabrication was carried out as specified in the drawings with minor adjustments to the dimensions

1. Fuselage and Gear Plates: The Fuselage is a crucial component that must be lightweight and durable enough to withstand impacts (Debiasi 2020). A template was made by using straw board to the scale of the drawings for both fuselage and gear plates. A mould was created for the casting in acrylic, the mixture for the cast was now poured into the mould and allowed to be solidified. After the cast is solidified, it was brought out of the mould and allowed to dry on a flat surface, and subsequently spray painted shown in Figure 2. The rods were subsequently welded together, and the wing tips trimmed to fit the marked-out pattern. The total wingspan is 1.234 m, with a surface area of 0.566 m^2 for each wing as shown in Figure 3.
   figure 3.

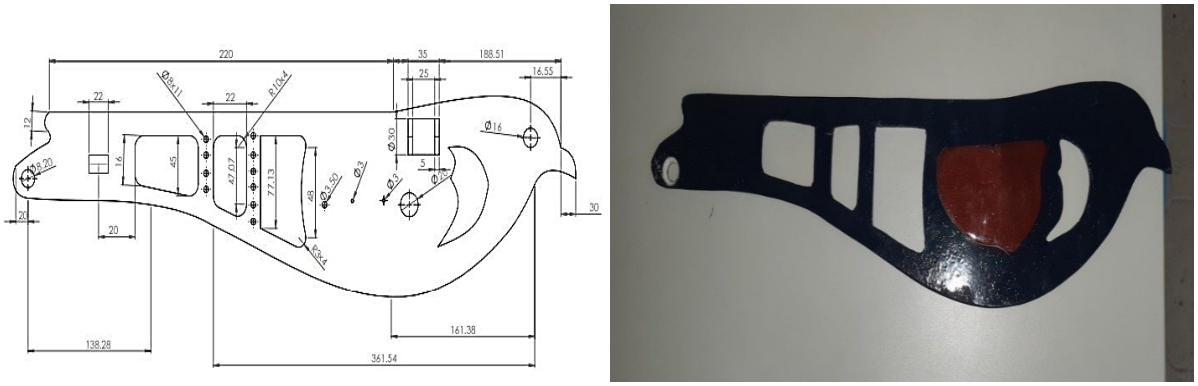

Figure 2a: Solidworks Drawing of Fuselage with Dimensions, Fig 2b: Finished Fuselage and Gear Plates

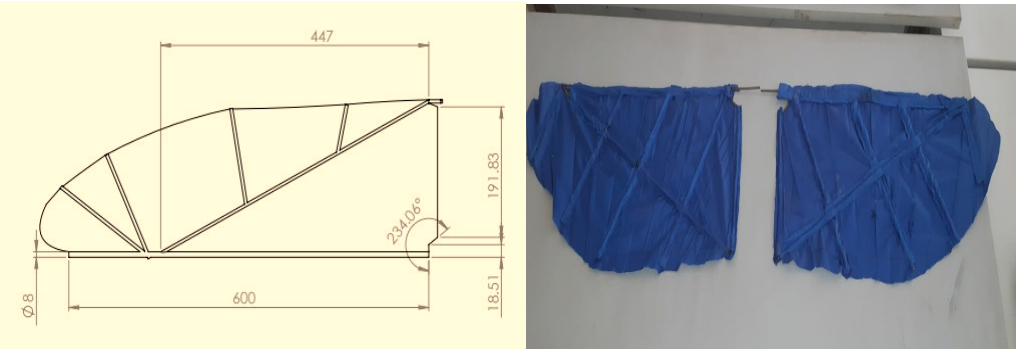

Figure 3a. Solidwork Drawing Of Wing with Dimensions, Figure 3 b. Finished Wings

2. Flapping Mechanism: Shaft was fabricated using two circular wooden disks, a hollow aluminum rod and two cranks of length 8cm and a plastic gear. These were put on the bird individually during assembly process as shown in Figure 4.

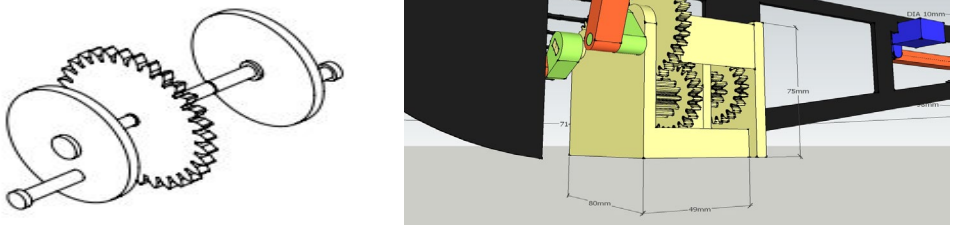

Figure 4. SolidWorks Isometric Rendering for Transverse Transmission Shaft

3. Wing Hinge and Holder: The wing hinge was cut from the metal sheet 12cm by 4cm and the folded into 4cm off the edges. The edges were then trimmed, and the ball bearings inserted into the folds in holes which were created by using the oxy welding flame and held inside by using epoxy gum. Two hinges were made and the wing holder was crafted from wood and made to fit into the hinge as shown in Figure 5a and 5b.

Figure 5a. Wing Housing

Figure 5b. Finished Hinge

4. Power Source: Motor: The model is powered by an A2212/13T Brushless Outrunner DC Motor. Brushless motors are typically 85-90% efficient whereas brushed DC motors are around 75-80% efficient. This difference in efficiency means that more of the total power used by the motor is being turned into rotational force and less is being lost as heat. This motor has a 2200KV (rpm/v) rpm rating and can pull max of 21.5A current at 11.1V. So, it is capable to deliver 239W maximum power output under loaded condition and turns at a rate of 24,642rpm at no load at 100% throttle. The outer magnet can rotate, and the coil remains stationary as shown in Figure 6a. This motor's speed is controlled by a HK SS Series brushless 40A electronic speed controller as shown in Figure 6b. It gives a 40A burst for 10 seconds and 30A continuous. Lithium polymer batteries provide high energy storage to weight ratios in an endless variety of shapes and sizes (Akande et al. 2021). The 25C 2200mAh 3S Lipo battery used is shown in Figure 6c. MC6 2.4GHz 6 channel transmitter and receiver control was used as shown in Figure 6d, the MC Series offers great performance, excellent range and reliability. The

Microprocessor constantly scans for the best available channel to provide a care free flying experience without any transmission issues.

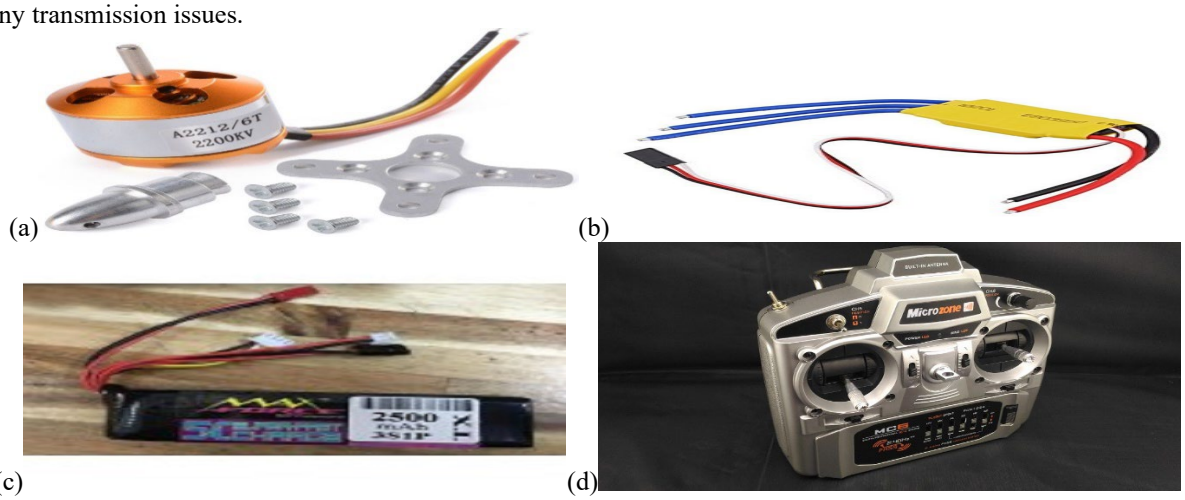

(a) (b) (c) (d)

Figure 6a: A2212/13T Brushless Outrunner Motor, Figure 6b: Electronic Speed Controller, Fig 6c: 25C 2200mAh 3S Lipo Battery, Figure 6d: MC-6C 2.4GHz 6 channel transmitter and receiver

Electrical Configuration and Circuit: To ensure control of thrust, sideways, downward and upward movement of the model, the electrical components (ESC, two servos) are connected to the RC receiver. In total 3 channels are needed to control the model bird. The ESC is simply connected to the motor, which is the thrust channel of the receiver and the two servos are connected to channels one and two of receiver module. As the frequency of the transmitter is very high, its antenna is small in contrast with the AM/FM transmitter and the antenna has a null region on the area pointed by the antenna tip (Adetunla 2020). So, for better controlling, the antenna tip was made sure it wont point at the direction of the model during flight time, while the ESC has a battery eliminating circuit, which helps to power up the receiver module and also the servos. Also, a low voltage cut-off was installed to prevent damage of the Li-po battery that powers the whole system. The use Raspberry pi which has Bluetooth and Wi-Fi to enable streaming of exergy Analysis data from sensors to a mobile device was employed. The receiver Receives power from the battery which is directly connected to the servos for the tail movement and also connected to the ESC as shown in Figure 7.

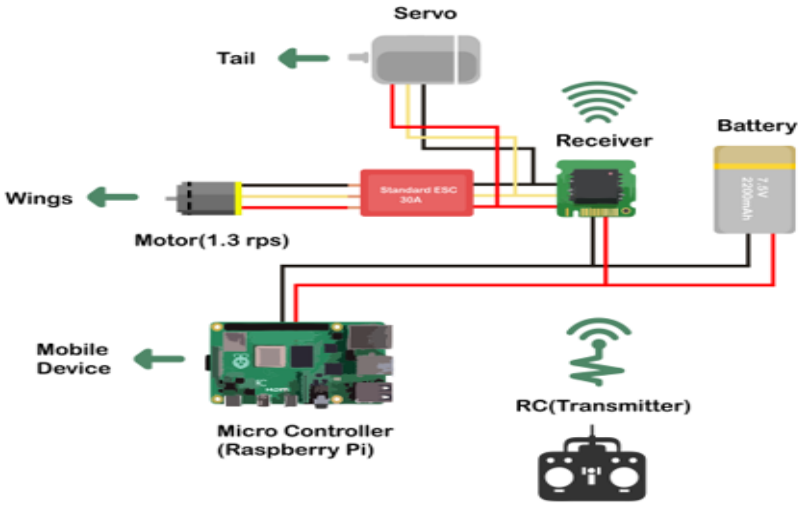

Figure 7. Hardware connection of the model.

5. Wings and Tail: The skeleton of the wings and the tail was made using oxy electrodes and aluminium sheets were used to hold in the electrodes for the tail (figure 7). A template was created by using cardboard to scale of the wing drawing. The carbon was beaten off the electrodes.

4. Results and Discussion

4.1 Aerofoil Simulation

The aerodynamic behaviour of the selected aerofoil NACA741 was simulated and studied. For the simulation, a 1000mm long section of the wing was placed in a 3m/s air stream, with an angle of attack of 5 degrees. The simulation successfully generated the following output data are shown in Table 2.

Table 2. Aerofoil Neutral Position Aerodynamic Simulation Output Data

Output	Unit	Value
Lift force	N	0.811
Drag force	N	0.200
Coefficient of lift		0.589
Coefficient of drag		0.145

Figure 8 shows that the velocity profile of air above the aerofoil is greater than the velocity below the aerofoil, which is one of the primary conditions necessary for lift generation.

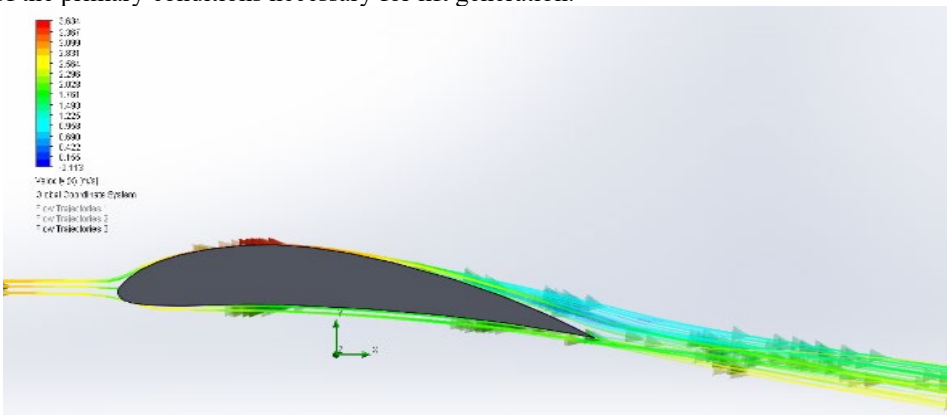

Figure 8. Simulated Air Flow Around Aerofoil Section (Velocity)

Figure 9 shows that the air pressure above the aerofoil is less than the velocity below the aerofoil, which is also a primary conditions necessary for lift generation. As both conditions have been met, the aerofoil was integrated into the design.

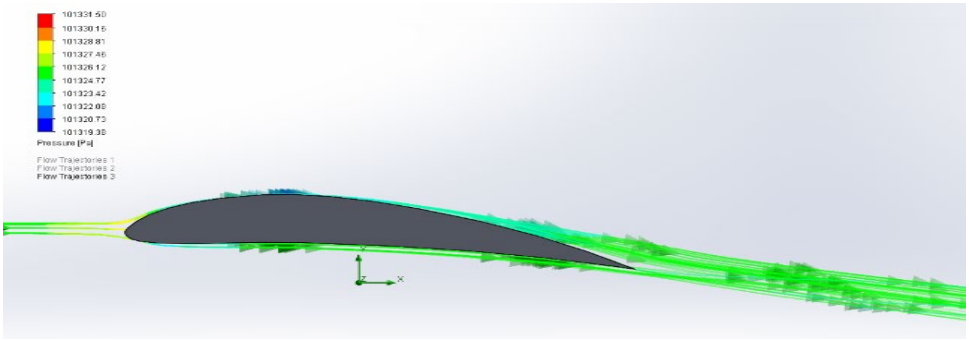

Figure 9. Simulated Air Flow Around Aerofoil Section (Pressure)

The simulation was repeated for various angles of attack ranging from 0 to 35 degrees. These simulations produced the results in Table 3 and were used to plot graphs in Figure 10, which shows the relationship between Lift Coefficient, Drag Coefficient and angle of attack also known as the Lift and Drag Curve Slope.

Table 3. Aerofoil Aerodynamic Simulation with Varying Angle of Attack Output Data

Angle of attack (°)	Lift force (N)	Drag force (N)	Lift Coefficient	Drag Coefficient
0	0.354	0.146	0.257	0.106
5	0.811	0.2	0.589	0.145
10	1.158	0.31	0.84	0.225
15	1.49	0.435	1.082	0.316
20	1.421	0.838	1.03	0.608
25	2.009	0.872	1.458	0.633
30	1.727	1.136	1.253	0.824
35	1.567	1.505	1.137	1.092

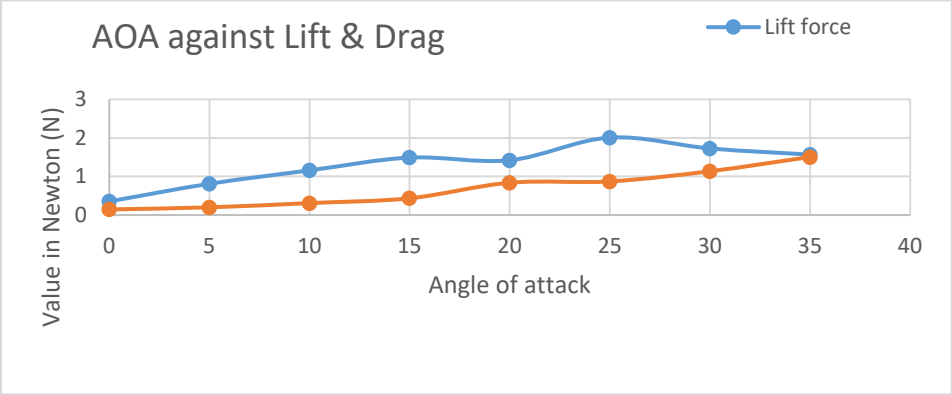

Figure 10. The Relationship between Lift, Drag and Angle of Attack

This Graph validates the choice of the aerofoil because compared to other aerofoils, the slope of the graph is high (Baneshi 2021). The data generated from the simulation shows that the aerofoil begins to stall at an angle of 25 degrees, this means there is a reduction in lift generated from the point. The fluid flow trajectory at the stall point is shown in Figure 11.

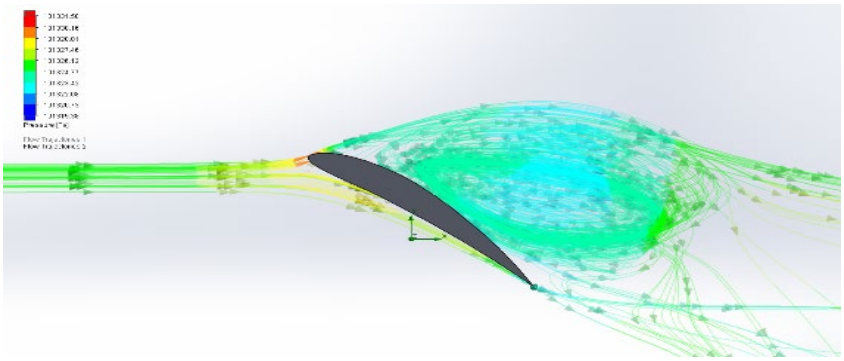

Figure 11. Aerofoil Simulation at 25 Degrees

4.2 Aerodynamic of the Ornithopter's Tail

The aerodynamics of the vertical stabilizer of the tail was simulated by using SolidWorks 2016 flow simulator. For the simulation, an accurate 3d model of the Ornithopter tail placed in a 3m/s air stream, at its maximum angle of 15 degrees (Akande et al. 2021). The simulation was done to determine accurately the turning force and drag force exerted on the tail by the wind. Table 4 shows the values obtained.

Table 4. Tail Aerodynamic Simulation Output Data

Output (N)	Value	Minimum Value	Maximum Value	Averaged Value
Drag	0.029332741	0.029248855	0.030146473	0.029741314
Force (Y)	-0.088336854	-0.091534635	-0.088027001	-0.089962773

The negative sign of the forces indicates that the forces acting on the tail are in a negative Y direction (downward). Figure 12 shows the air flow trajectory over the horizontal stabilizer of the tail.

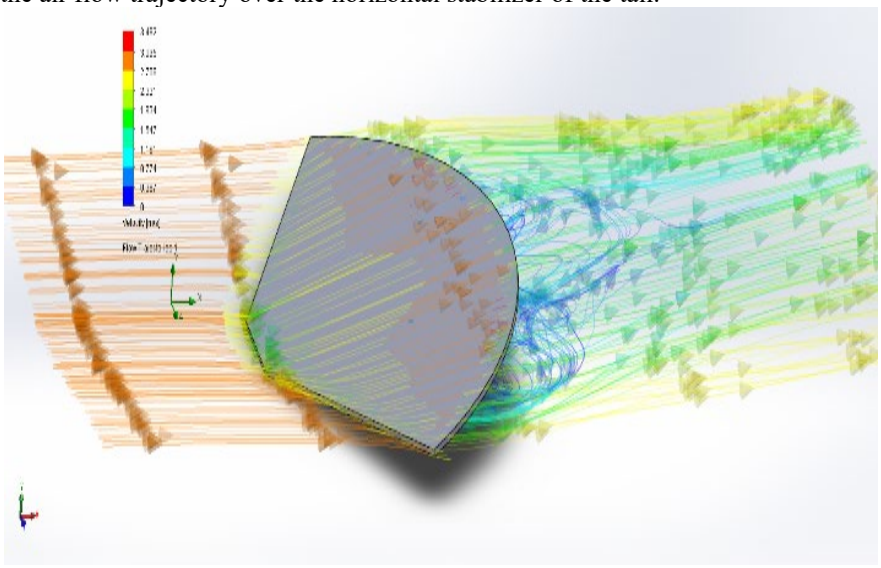

Figure 12. Aerodynamic Simulation of Horizontal Stabilizer at 5 Degrees.

4. 3 Aerodynamic Simulation of Ornithopter

The pictorial results of flow simulation of the Ornithopter is shown in Figure 13. For the simulation, a 3d model of the Ornithopter was placed in a 5 m/s air stream, with an angle of attack of 5 degrees. The simulation successfully generated the following output data shown in Table 5.

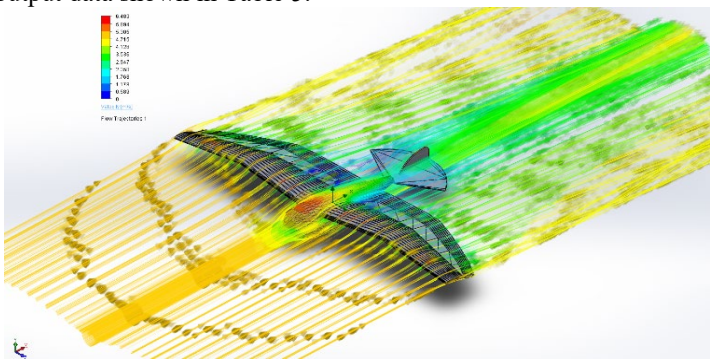

Figure 2. Aerodynamic Simulation of Ornithopter Model

Table 5. Ornithopter Aerodynamic Simulation Output Data

Parameter	Value	Minimum Value	Maximum Value	Averaged Value

Drag Force (N)	0.601239474	0.599640774	0.604090165	0.60134382
Lift Force (N)	2.701223899	2.69085547	2.711809909	2.698637009
Lift coefficient	1.960071763	1.952548187	1.967753222	1.958194655
Drag Coefficient	0.436273541	0.435113487	0.43834207	0.436349257

The data shows that the Ornithopter will be able to produce an upward force of 2.7 N at 5m/s without assistance from flapping.

5. Conclusion

The study offers an overview of the basic principles of the design of Ornithopters. The first prototype of ornithopter was flown for less than 1 min in Dec, 2004. Its wingspan was about 40 cm and weighed around 45 g. This research succeeded in increasing its size to 124 cm and its weight to almost 2000 g, which is similar to the average weight of a bird, therefore, ensuring that the developed Ornithopter fly in wind velocity of over 5m·s−1. In this paper, the aerodynamic behavior of the developed Ornithopter was characterized through experiment and simulation. It was evident that the aerodynamic model utilized agrees well with experimental data especially in regions of high angle of attack and dynamic-stall effects with no plunging motion. The findings presented in this paper could further increase the applicability of Unmanned Aerial Vehicles in Manufacturing Industries.

References

Akande, S., A. Adetunla, T. Olanrewaju, and A. Adeoye, UAV and Its Approach in Oil and Gas Pipeline Leakage Detection, vol. 20, pp 231, 2021.

Adetunla A. and E. . Akinlabi, Finite Element Analysis of the Heat Generated During FSP of 1100 Al Alloy, *Lect. Notes Mech. Eng.*, pp. 425-431, 2020.

Abel, Design and Feasibility Study of Personal Ornithopters, 2014.

Baneshi N.., Investigation the mechanical properties of a novel 3D multicomponent scaffold coated with a new bio-nanocomposite for bone tissue engineering: Fabrication, simulation and characterization, *J. Mater. Res. Technol.*, vol. 15, pp. 5526–5539, 2021Bento, P. Air, and F. Academy, “Unmanned Aerial Vehicles : An Overview, no. January 2008, 2017.

Bhargava and A. Bhargava, Ornithopter design and operation vol. 1, pp. 64–67, 2014.

Bhargava, A. Bhargava, and S. K. Jangid, Ornithopter Development and Operation, no. March, 2015.

Box, A Review on Bio-Inspired Ornithopter Sharath, vol. 5, no. 05, pp. 474–479, 2017.

De Croon, M. A. Groen, C. De Wagter, B. Remes, R. Ruijsink, and B. W. Van Oudheusden, Design , Aerodynamics , and Autonomy of the DelFly, no. 2, pp. 1–36, 2009.

Dubey I. and M. Amir, A small unmanned flapping airvehicle ‘Ornithopter, vol. 8, no. 9, 2017.

Debiasi, M and .Low-Noise, Flapping Wings with Tensed Membrane, vol. 58, no. 6, pp. 2388–2397, 2020.

Jackowski Z. J.and Z. J. Jackowski, Design and Construction of an Autonomous Ornithopter by, 2009.

Kumar, P. Kumar, S. Singh, and A. Reddy, Design & Analysis of Ornithopter, vol. 8, no. 3, pp. 217–226, 2020.

Meiser, V., R. Henke, D. Šeatović, and M. Systems, Autonomous Unmanned Ground Vehicle as Sensor Carrier for Agricultural Survey Tasks, pp. 6–10, 2014.

Percin M. , First free-flight flow visualisation of a flapping-wing robot, pp. 1–30, 2015.

Rawat, U. A. Pawar, S. Roy, and R. Swami, A Designing Approach for a Flapping Wing Micro Air, pp. 7–13, 2013.

Singhal, G., Unmanned Aerial Vehicle Classification , Applications and Challenges : A Unmanned Aerial Vehicle classification , Applications and challenges : A Review, no. November, 2018..

Srigrarom and W. Chan, Ornithopter Type Flapping Wings for Autonomous Micro Air Vehicles, pp. 235–278, 2015.